PHYSICAL SCIENCE

Critical impact of vegetation physiology on the continental hydrologic cycle in response to increasing CO_2

Léo Lemordant[a]*, Pierre Gentine[a,b], Abigail Swann[c,d], Benjamin I. Cook[e,f], Jacob Scheff[f]

[a]Earth and Environmental Engineering Department, Columbia University, 500 W. 120th St, 918 S. W. Mudd Hall, 500, New York, NY 10027, USA

[b]Earth Institute, Columbia University, 2910 Broadway, New York, NY 10025, USA

[c]Department of Atmospheric Sciences, University of Washington, Building Box 351640, Seattle, Washington, USA

[d]Department of Biology, University of Washington, 24 Kincaid Hall Box 351800, Seattle, Washington, USA

[e]NASA Goddard Institute for Space Studies, 2880 Broadway, New York, NY 10025, USA

[f]Ocean and Climate Physics, Lamont-Doherty Earth Observatory, Palisades, NY, 10964, USA

*Correspondence: Léo Lemordant – leo.lemordant@columbia.edu or Pierre Gentine – pg2328@columbia.edu

Supplementary Information: Figure Legends

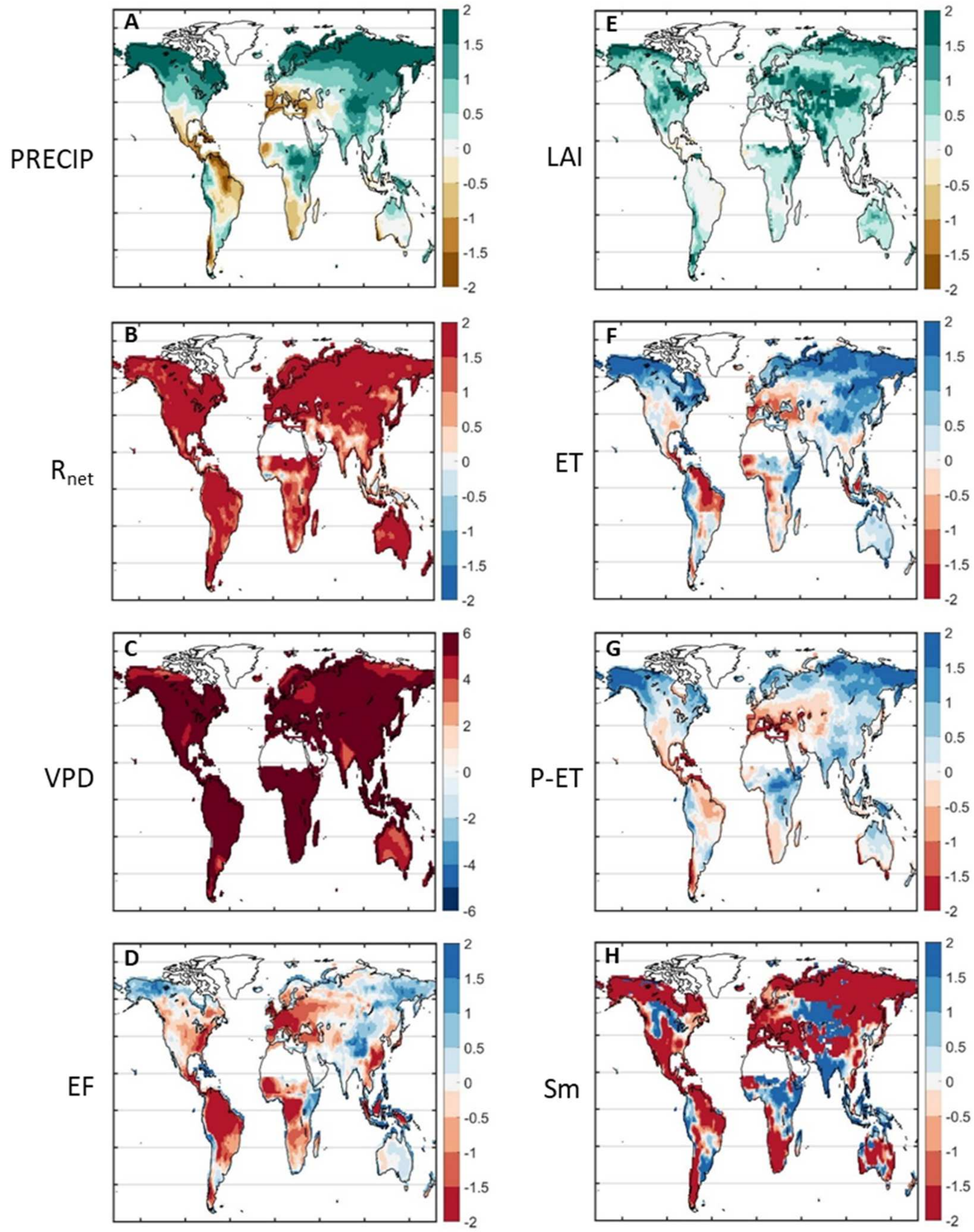

Figure S1. Standardized changes in RCP 8.5 with all forcings (land use and land cover change, aerosols, ozone, etc…) of precipitation (**A**), net radiation (**B**), VPD (**C**), EF (**D**), LAI (**E**), ET (**F**), P-ET (**G**) and soil moisture at 2m (**H**). Change is quantified by the difference of the years 89-118 of the simulation and the years 1-20, normalized by the standard deviation of CTRL over the years 1-20 (Methods).

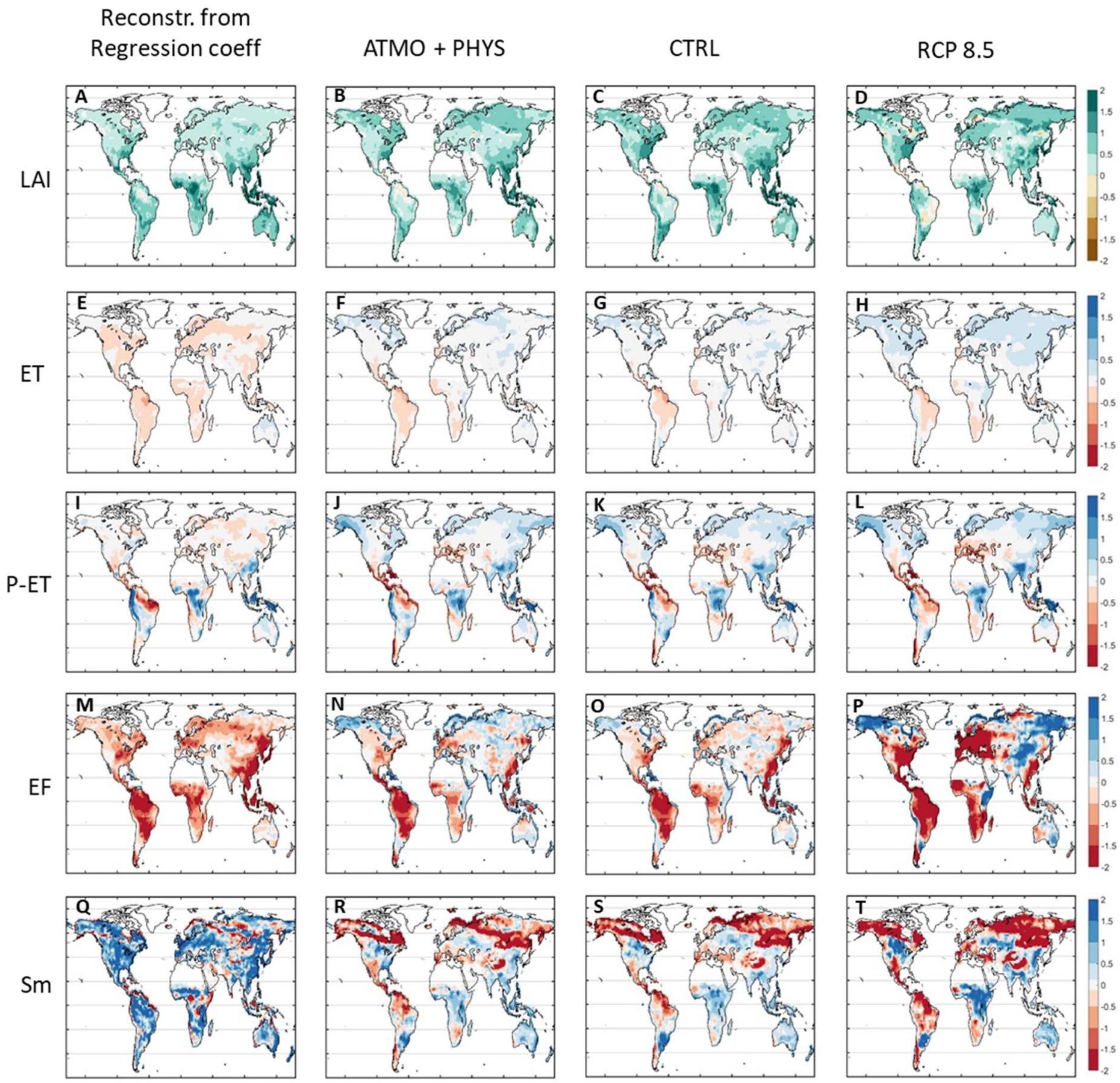

Figure S2. Reconstruction of the change (difference between years 89-118 and years 1-20) from the multiple linear regression (first column), the addition of changes in ATMO and PHYS (second column), and the comparison with CTRL (third column) and RCP 8.5 (fourth column) for LAI (**A**, **B**, **C**, **D**), P-ET (**E**, **F**, **G**, **H**), EF (**I**, **J**, **K**, **L**), and SM_{2m} (**M**, **N**, **O**, **P**).

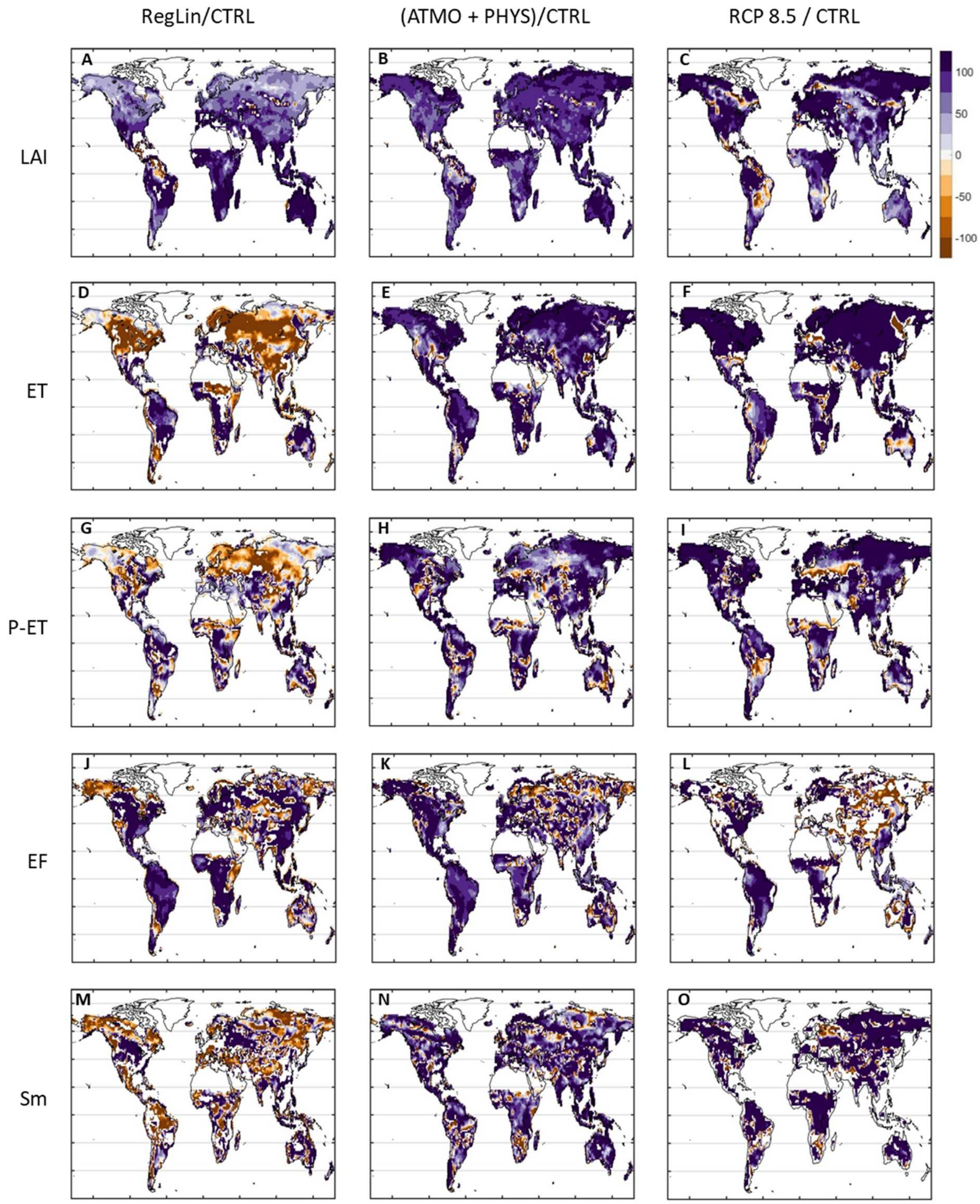

Figure S3. Reconstruction of the change (difference between years 89-118 and years 1-20) from the multiple linear regression (first column), the addition of changes in ATMO and PHYS (second column), and the comparison with CTRL (third column) and RCP 8.5 (fourth column) for LAI (**A**, **B**, **C**), ET (**D**, **E**, **F**), P-ET (**G**, **H**, **I**), EF (**J**, **K**, **L**) and SM_{2m} (**M**, **N**, **O**).

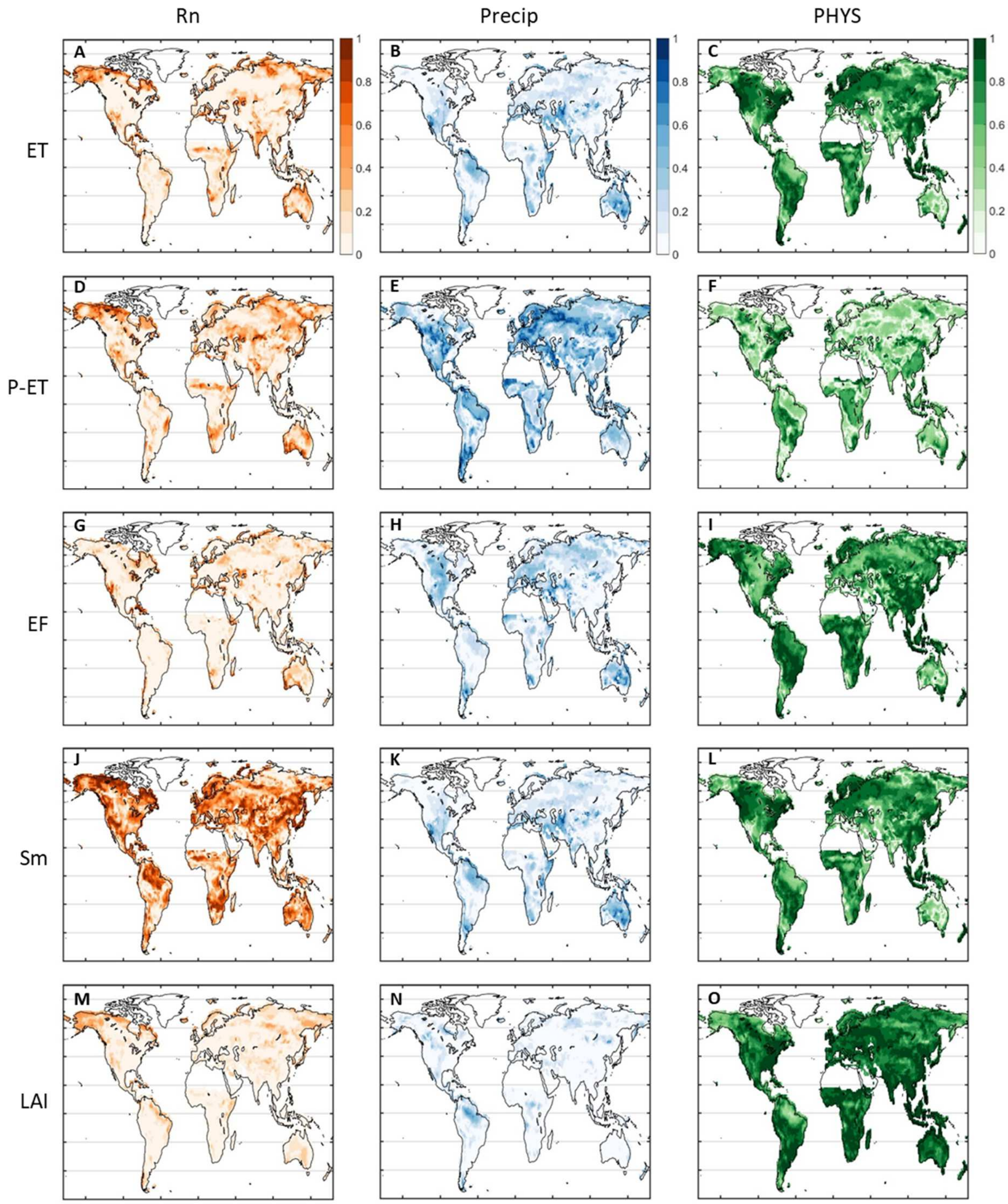

Figure S4. Individual contribution of net radiation to ET (**A**), P-ET (**D**), EF (**G**), Sm (**J**) and LAI (**M**) in CTRL according the decomposition. Individual contribution of precipitation to ET (**B**), P-ET (**E**), EF (**H**), Sm (**K**) and LAI (**N**) in CTRL. Individual contribution of physiological effects to ET (**C**), P-ET (**F**), EF (**I**), Sm (**L**) and LAI (**O**) in CTRL**.**

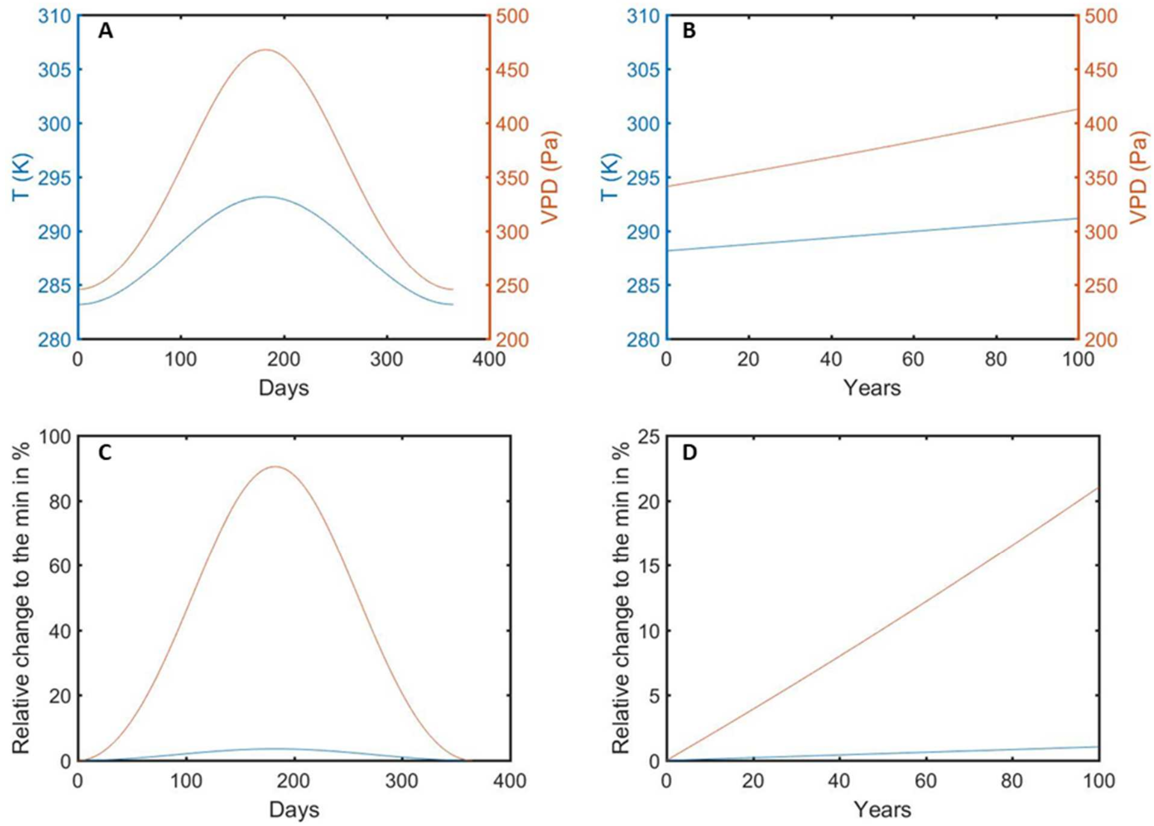

Figure S5. The VPD exponential dependence on temperature alone explains that a 3K temperature variations, or less than 10% change, lead to large seasonal (**A**) and long run climate change (**B**) variations of VPD, dozens of percent variations relatively to the minimum (**C** and **D** respectively). Relative humidity is kept constant at 80%.

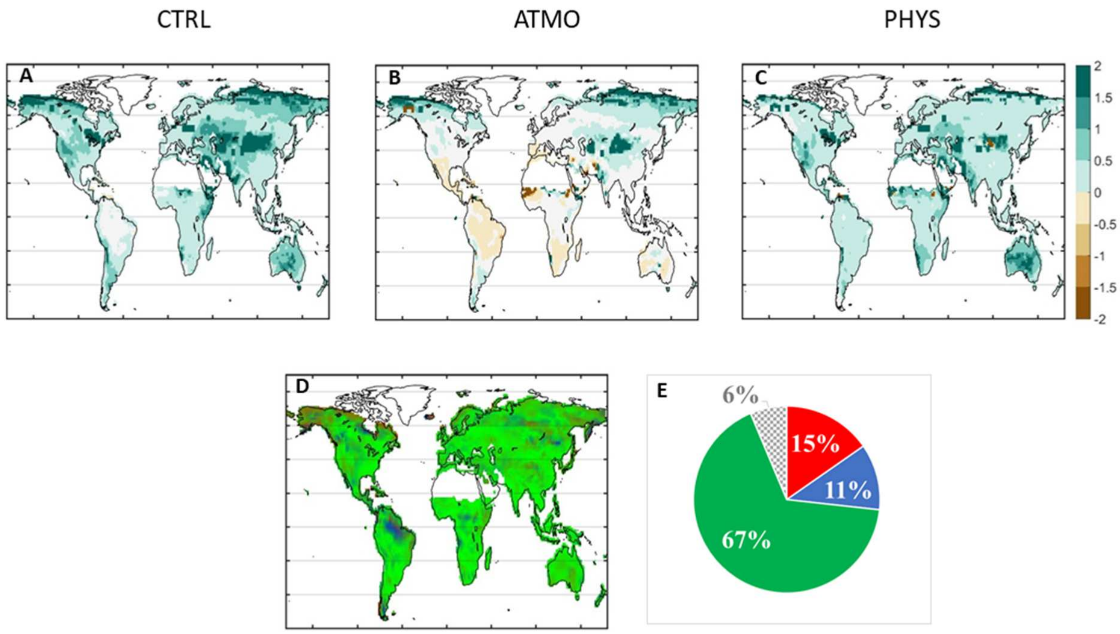

Figure S6. LAI (annual) changes in CTRL (**A**), ATMO (**B**), and PHYS (**C**) runs, are quantified by the difference of the years 89-118 of the simulation and the years 1-20, normalized by the standard deviation of CTRL over the years 1-20 (Methods). For the decomposition along the three main drivers of LAI (**D**), Green quantifies the effect of the vegetation physiology based on the run PHYS; red and blue quantify the contribution of, respectively, net radiation and precipitation, based on a multiple linear regression of ATMO. The pie chart (**E**) shows for each variable the global average of each contribution, weighted by the total effect including error terms, reported as a grey shaded area.

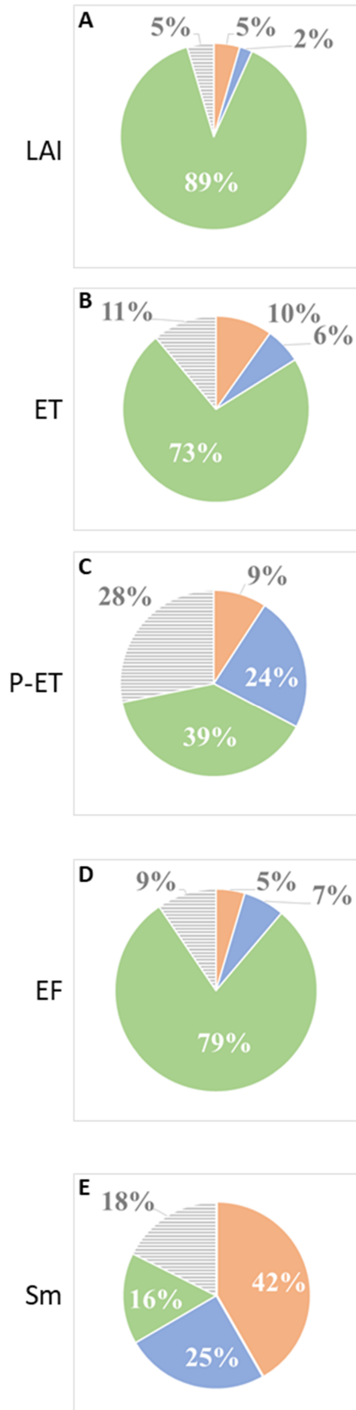

Figure S7. After the decomposition along the three main drivers of LAI (**A**), ET (**B**), P-ET (**C**), EF (**D**), Soil moisture at 2m (**E**) in CTRL, the pie charts show for each variable the fraction (labelled in %) of land under the main influence (more than 50% of the changes is attributed to this driver) of one the three main drivers (green for grid points dominated by vegetation physiology, red for grid points dominated by net radiation, and blue for grid points dominated by the precipitation), and under no single driver influence (dashed area).

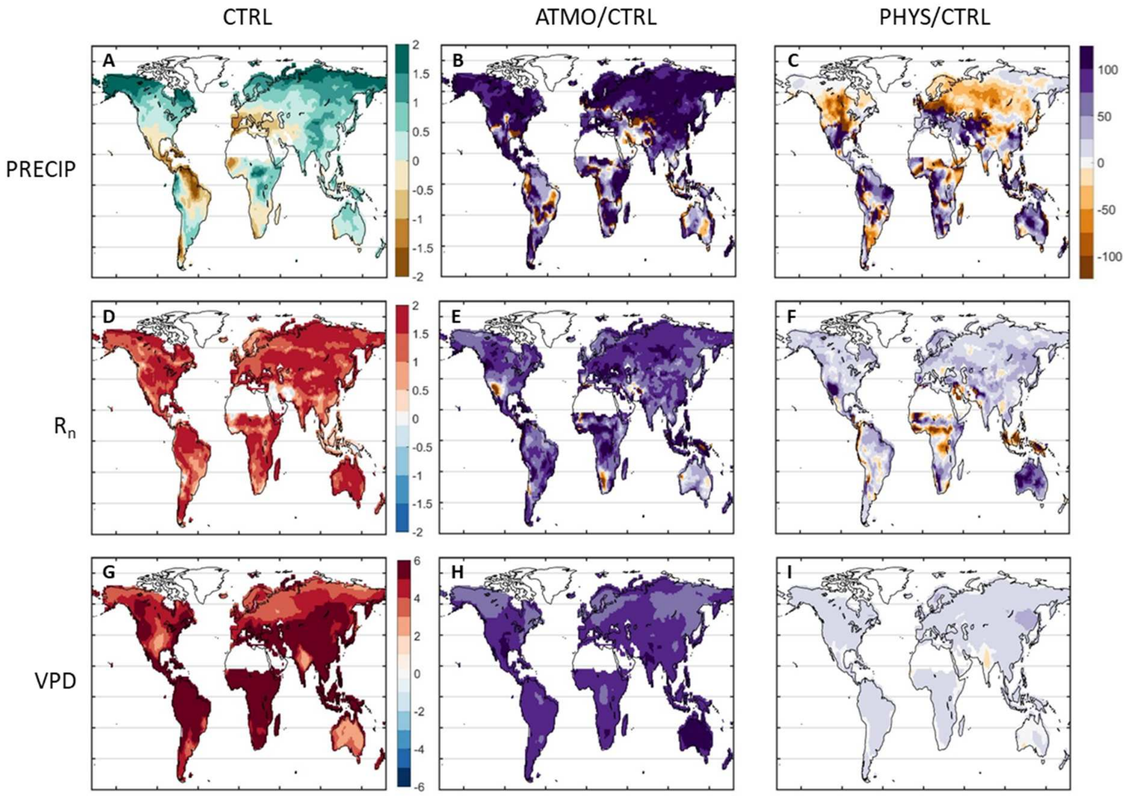

Figure S8. Precipitation (**A**, **B**, **C**; annual), Net radiation (**D**, **E, F**; annual) and VPD (**G**, **H**, **I**; growing season) are presented. The left column shows results for CTRL as changes normalized by the standard deviation of CTRL over the years 1-20 (Methods), whereas the center and right columns show the changes of ATMO and PHYS relative to the changes of CTRL in % (purple to orange colorbar). Change is quantified by the difference of the years 89-118 of the simulation and the years 1-20. The changes observed for VPD are much larger in amplitude than for R_n and P, so that the scale was adjusted accordingly for VPD in G.

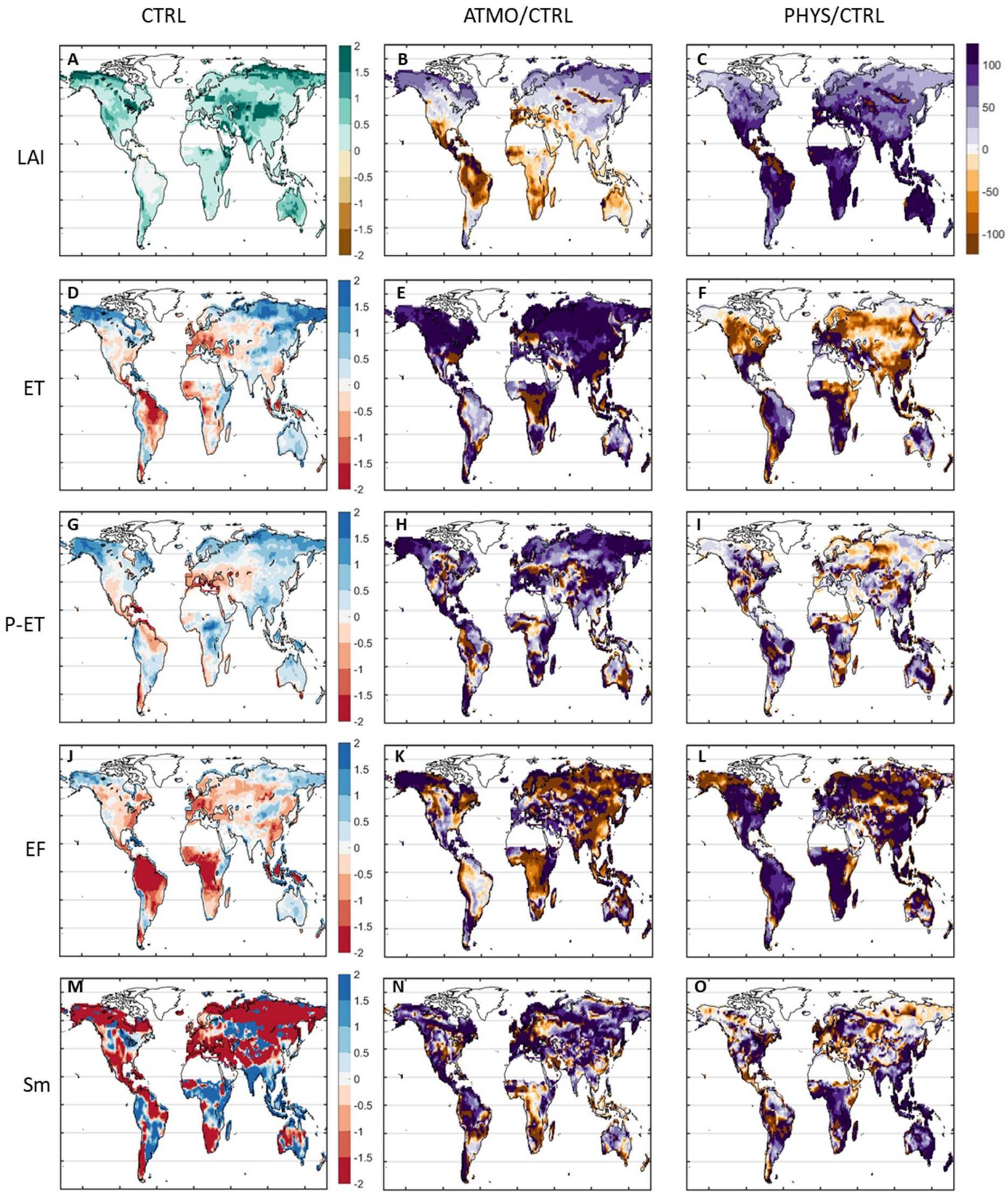

Figure S9. LAI (**A**, **B**, **C**; annual), ET (**D**, **E**, **F**; annual), P-ET (**G**, **H**, **I**; annual), EF (**J**, **K**, **L**; growing season), soil moisture at 2m (**M**, **N**, **O**; growing season) changes are shown on the left column for CTRL, normalized by the standard deviation of CTRL over the years 1-20 (Methods). The center and right columns show the changes of ATMO and PHYS relative to the changes of CTRL in % (purple to orange colorbar).

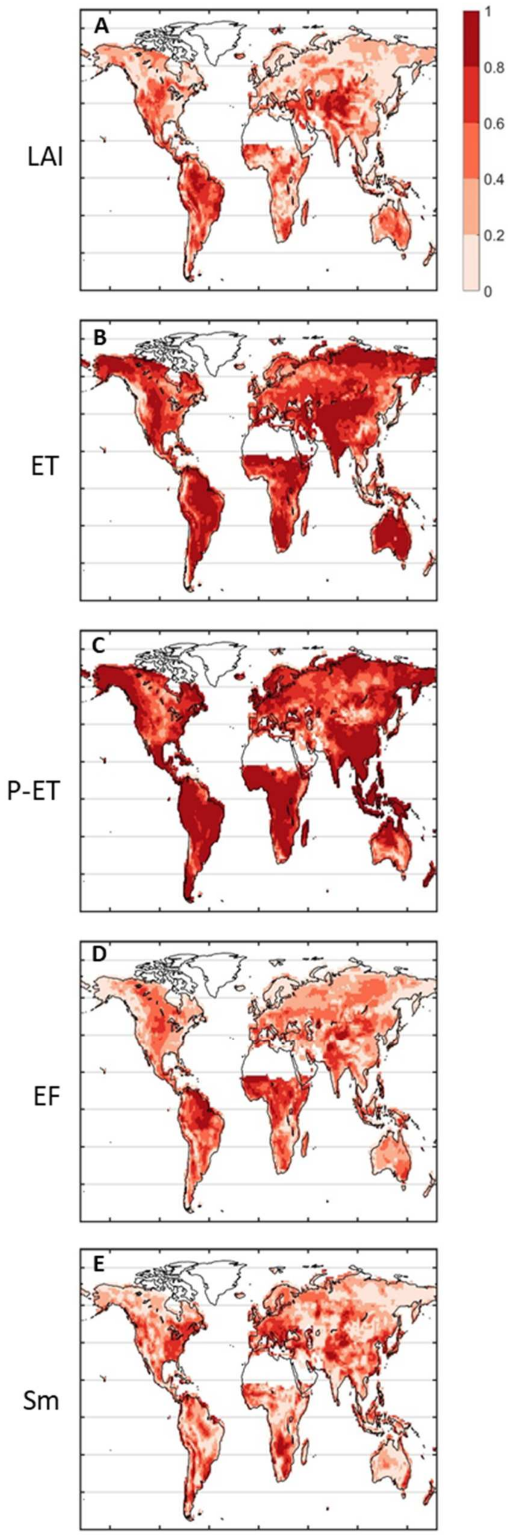

Figure S10. Fraction of variance explained by the multiple linear regression (R^2) for LAI (**A**), ET (**B**), P-ET (**C**), EF (**D**), SM_{2m} (**E**).

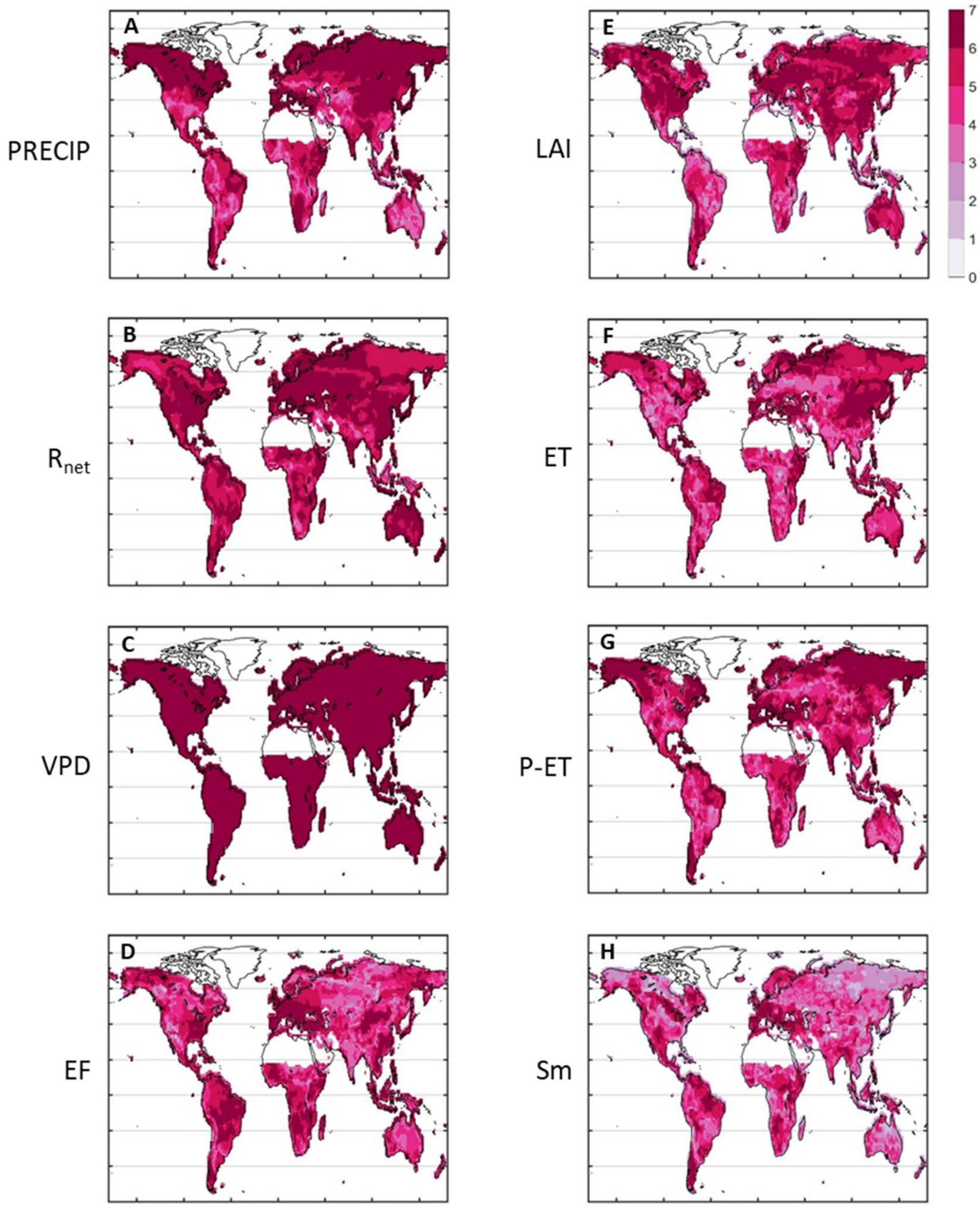

Figure S11. Numbers of models that agree with the inter-model average sign from 1 to 6, for Precipitation (**A**), R_n (**B**), VPD (**C**), EF (**D**), LAI (**E**), ET (**F**), P-ET (**G**), SM_{2m} (**H**).

	1pctCO2		RCP 8.5	
historic period	1850	1869	1941	1970
historic years id	*1*	*20*	*91*	*120*
historic $[CO_2]$ min-max (ppm)	284	347	310	325
historic $[CO_2]$ average (ppm)	313		315	
future years	1939	1968	2070	2099
future years id	*89*	*118*	*220*	*249*
future $[CO_2]$ min-max (ppm)	690	920	670	927
future $[CO_2]$ average (ppm)	800		799	

Table S1. Years considered for temporal averaging to match similar levels of $[CO_2]$ in 1pctCO2 runs